Available online at www.sciencedirect.com
ScienceDirect
Journal of Power Sources 174 (2007) 493–500
JOURNAL OF POWER SOURCES
www.elsevier.com/locate/jpowsour

# Effect of carbonaceous materials on electrochemical properties of nano-sized $Fe_2O_3$-loaded carbon as a lithium battery negative electrode

Bui Thi Hang [a,*], Takayuki Doi [b], Shigeto Okada [b], Jun-ichi Yamaki [b]

[a] *Japan Science and Technology Agency, Kasuga Koen 6-1, Kasuga 816-8580, Japan*
[b] *Institute for Materials Chemistry and Engineering, Kyushu University, Kasuga Koen 6-1, Kasuga 816-8580, Japan*

Available online 22 June 2007

**Abstract**

Nano-sized $Fe_2O_3$-loaded carbon material was prepared by loading $Fe_2O_3$ on carbon using various carbonaceous materials. Carbonaceous materials strongly affected the electrochemical behavior of nano-sized $Fe_2O_3$-loaded carbon. Among the carbons used, nano-carbons such as acetylene black (AB), tubular carbon nanofibers (CNF), and platelet CNF provided larger capacities than other carbons. This may be due to the greater surface area of nano-carbon, which gives a greater distribution of nano-sized $Fe_2O_3$ particles than other carbons and delivers a greater capacity than other carbons. Investigation of the first-cycle materials by X-ray photoelectron spectroscopy (XPS) revealed that $Fe_2O_3$ was reduced to Fe metal in the charge process (reduction of $Fe_2O_3$), and, conversely, Fe metal was not completely oxidized to $Fe_2O_3$ during discharge (oxidation of Fe). This result may be due to the covering of non-conductive $Li_2O$ formed during charging.


*Keywords:* Nano-sized $Fe_2O_3$-loaded carbon material; Lithium battery anode

## 1. Introduction

Iron oxides have been reported to act as active materials in lithium batteries [1–3]. Lithium reacts with iron oxides to give $Li_2O$ and metallic iron through various intermediate phases such as $LiFe_5O_8$, $LiFeO_2$ and $Li_5FeO_4$ [1,4]. However, a problem with this material is that its irreversible phase-transformation during the reaction [2,3] limits its utilization. The effect of particle size of the iron oxide on lithium intercalation into α-$Fe_2O_3$ particles was demonstrated by Larcher et al. [4,5]. Higher capacity could be obtained in $Fe_2O_3$ nano-particles than in $Fe_2O_3$ micro-particles. Therefore, the particle size and surface area of the iron oxide influence the cycle performance of the electrode. Recently, some iron oxides with nano-sized particles have been reported to react with lithium as a reversible material [4–8]. However, the capacity of nano-size $Fe_2O_3$ decreased rapidly with repeated cycling. To obtain high capacity by increasing the surface area and decreasing the particle size of $Fe_2O_3$, nano-sized $Fe_2O_3$-loaded carbon was prepared. In our previous work [9], we found that nano-sized $Fe_2O_3$-loaded AB and graphite act as rechargeable materials in a lithium battery. In this study, the effect of the morphology of various carbonaceous materials such as tubular carbon nanofibers (CNF), platelet CNF and vapor-grown carbon fibers (VGCF) on the electrochemical properties of nano-sized $Fe_2O_3$-loaded carbon were examined to find the most suitable carbon for a high-capacity lithium battery negative electrode.

## 2. Experimental

Vapor-grown carbon fibers (VGCF; Showa Denko Co.), acetylene black (AB, Denki Kagaku Co.) and natural graphite (Chuetsu Graphite Co.), with average diameters of ca. 200 nm, 100 nm and 18 μm, respectively, were used in the present work. In addition, two kinds of carbon nanofibers (CNFs), a nanotube type, with an average diameter of ca. 50 nm, and a platelet type, with an average diameter of ca. 150 nm, were also investigated.

For tubular CNF, graphene is aligned parallel to the fiber axis while in platelet CNF graphene is aligned perpendicular to the fiber axis. The main characteristics of the carbonaceous materials used are listed in Table 1. Iron nitrate (Wako Pure Chemical, Co.) was used as the iron source.

Nano-sized $Fe_2O_3$-loaded carbon material was prepared by loading $Fe_2O_3$ on carbon, as described below. $Fe(NO_3)_3$ was impregnated on carbon with an iron to carbon weight ratio

* Corresponding author.
*E-mail address:* hang@cm.kyushu-u.ac.jp (B.T. Hang).

0378-7753/$ – see front matter © 2007 Elsevier B.V. All rights reserved.
doi:10.1016/j.jpowsour.2007.06.031

Table 1
Main characteristics of the carbonaceous materials

| | Grain size (nm) | BET surface area ($m^2\ g^{-1}$) | True density ($g\ cm^{-3}$) |
|---|---|---|---|
| VGCF | 100–300 | 13 | 2.21 |
| AB | 40–100 | 68 | 2.0 |
| Natural graphite | 18000 | 8 | 2.24 |
| Tubular CNF | 20–100 | 92 | 2.09 |
| Platelet CNF | 40–200 | 91 | 2.10 |

of 1:8 in an aqueous solution, and the mixture was dried at 70 °C. This was followed by calcination for 1 h at 400 °C in flowing Ar. The iron compound obtained on the carbonaceous materials was identified to be $Fe_2O_3$ by X-ray diffraction (XRD). The actual weight ratio of iron to carbon in the obtained materials was checked by the polarized zeeman atomic absorption spectrophotometer (PZAAS) method. The morphology of the as-prepared nano-sized $Fe_2O_3$-loaded carbon materials was observed by transmission electron microscopy (TEM) using a TECNAI F20 and by scanning electron microscopy (SEM), together with X-ray energy dispersive spectroscopy (EDS) using a JSM-6060LA/VI (JEOL).

All electrochemical measurements were performed at 25 °C using a coin cell with lithium metal as a counter and a reference electrode. The working electrode was prepared by mixing 90 wt.% nano-sized $Fe_2O_3$-loaded carbon with 10 wt% polyvinylidene fluoride (PVdF) binder (KF#9100 from Kureha Chemical) dissolved in 1-methyl-2-pyrrolidinone (NMP). The slurry was coated onto the copper current collector. The coated films were dried and cut to 15 mm in diameter. To evaluate the

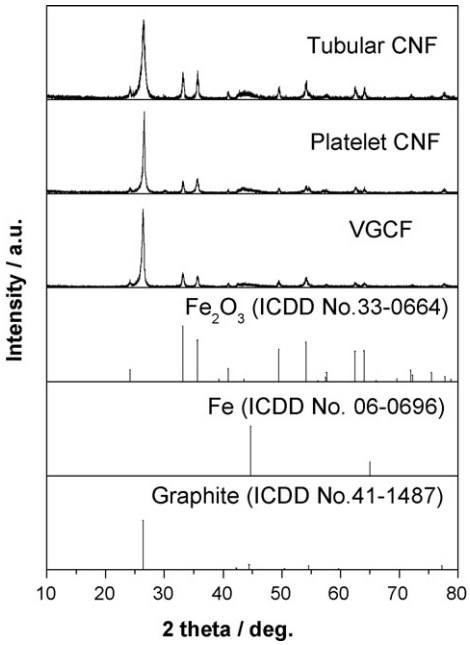


Fig. 1. X-ray pattern of the as-prepared nano-sized $Fe_2O_3$-loaded carbon.

contribution of carbon to the capacity of nano-sized $Fe_2O_3$-loaded carbons, carbon electrodes without $Fe_2O_3$ were prepared by the same procedure. A $Fe_2O_3$ electrode was also prepared with 90 wt% nano-sized $Fe_2O_3$ (Aldrich, ca. 3 nm) and 10 wt% PVdF binder for comparison with nano-sized $Fe_2O_3$-loaded carbon. These electrodes were then dried for 12 h at 120 °C in a vacuum oven. The cells were assembled in an argon-filled glove box. The electrolyte and separator were 1M $LiPF_6$ in EC-

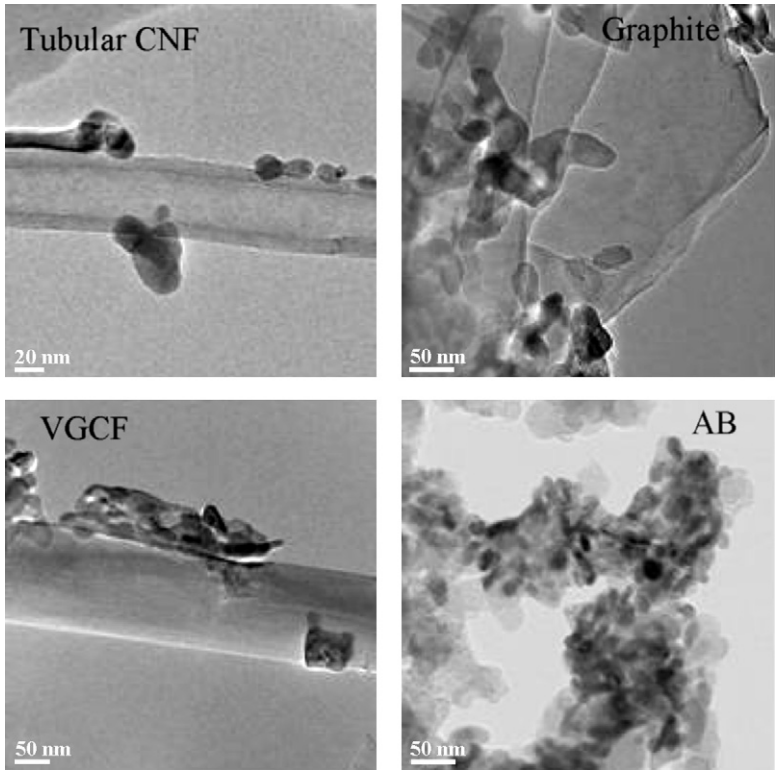


Fig. 2. TEM images of the as-prepared nano-sized $Fe_2O_3$-loaded carbon materials.

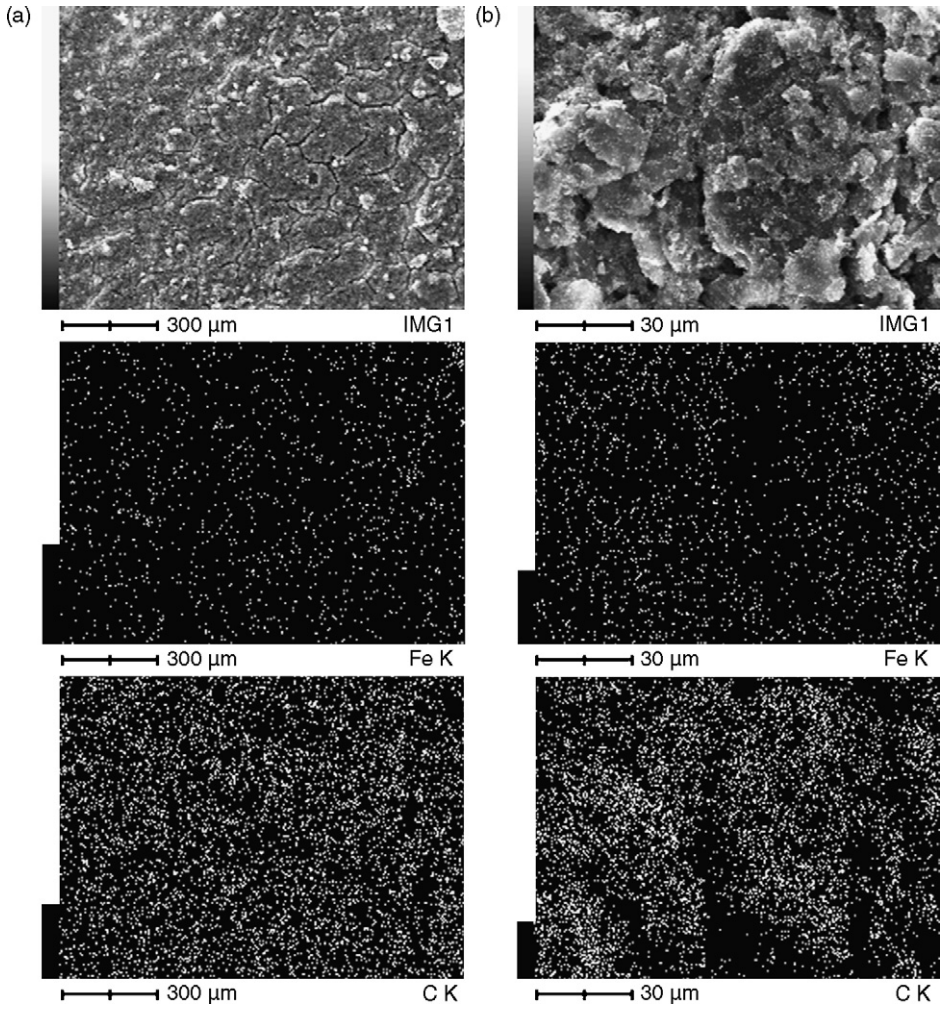


Fig. 3. SEM images and distribution of Fe and carbon for nano-sized $Fe_2O_3$-loaded (a) AB and (b) graphite before cycling.

DMC 1:1 by volume (Tomiyama Pure Chemical Co.) and porous polypropylene (Celgard #3501), respectively.

Cyclic voltammetry (CV) studies were carried out using an AutoLab instrument (ECO CHEMIE) at a scanning rate of 0.5 mV $s^{-1}$. Charge–discharge cycle tests of the coin cells were conducted at a constant current density of 0.2 mA $cm^{-2}$ and within a voltage range of 0.5–3.0 V using a cell-cycling device (NAGANO Co.).

To obtain the valence state of iron before and after cycling, X-ray Photoelectron Spectroscopy (XPS) analysis (JPS-9010 MC/IV, JOEL) was performed. After cycling, the coin cells were disassembled in a glove box filled with argon, and the working electrodes were washed with DMC solvent and then dried in a vacuum for 12 h. These electrodes were moved for XPS measurement using a transfer vessel. The X-ray source was a monochromatic $MgK_\alpha$ radiation system (10 kV, 10 mA).

## 3. Results and discussion

The X-ray patterns of the as-prepared material using various carbons are presented in Fig. 1. $Fe_2O_3$ particles are present on the carbon surface. Therefore, the active material in this case is $Fe_2O_3$.

For these preparation conditions, the weight ratio of iron to carbon is 1:8. To determine the actual amount of iron in the final product, the PZAAS method was used. The results showed that the actual weight ratio of iron to carbon in the obtained $Fe_2O_3$-loaded carbons was about 1:9.

To confirm the nature of the $Fe_2O_3$ present on the carbons, TEM measurements were carried out. TEM images of as-prepared $Fe_2O_3$-loaded carbons are shown in Fig. 2. The dark particles in this figure are $Fe_2O_3$. The TEM images demonstrated that fine $Fe_2O_3$ particles were dispersed on the carbon surface. The particle size of $Fe_2O_3$ is about a few tenths of a nanometer. $Fe_2O_3$ particles dispersed on tubular CNF and AB are smaller than those on graphite and VGCF. Such dispersion should increase the surface area of active material and improve the redox reaction of iron oxide.

Fig. 3 depicts SEM images and the distribution of iron and carbon by EDS of nano-sized $Fe_2O_3$-loaded carbon electrodes using AB and graphite, respectively. The distribution of iron and carbon on nano-sized $Fe_2O_3$-loaded AB and graphite electrodes revealed that iron particles were well dispersed on

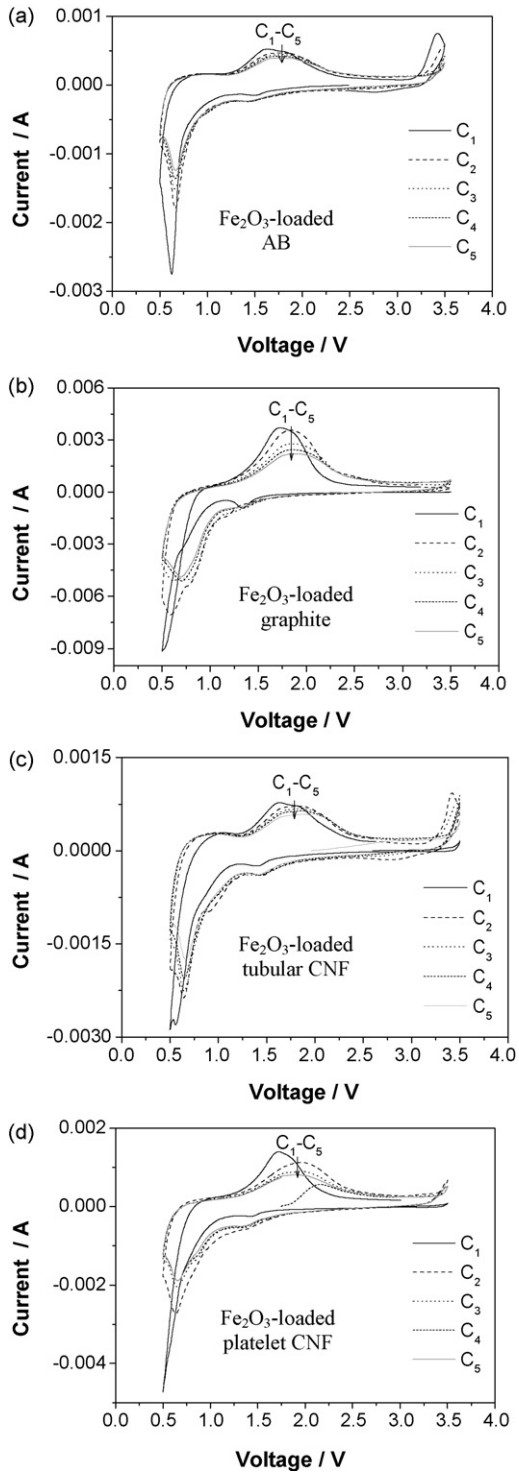


Fig. 4. Cyclic voltammograms for nano-sized $Fe_2O_3$-loaded carbon in the 5 initial cycles. Scan rate 0.5 mV $s^{-1}$.

the carbon surface. This distribution is expected to improve the cycle performance of nano-sized $Fe_2O_3$-loaded carbon electrodes.

Fig. 4 shows cyclic voltammograms for nano-sized $Fe_2O_3$-loaded carbons after 5 cycles. The CV curves of all electrodes clearly indicated a reversible reaction during reduction and oxidation with two peaks at around 1.5 V and 0.7 V upon reduction

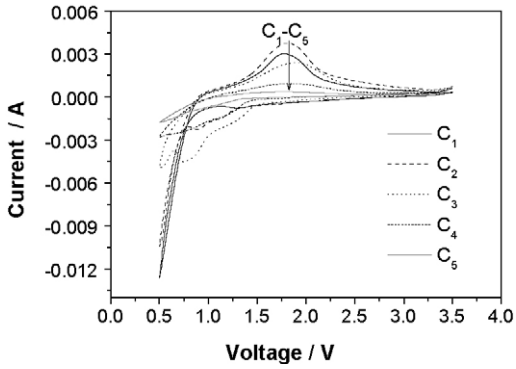


Fig. 5. Cyclic voltammograms for nano-sized $Fe_2O_3$ (Aldrich) without carbon in the 5 initial cycles. Scan rate 0.5 mV $s^{-1}$.

and one peak at around 1.8 V upon oxidation. This result suggests that nano-sized $Fe_2O_3$-loaded carbon acts as a rechargeable electrode material in a lithium battery. However, the currents gradually decreased during cycling, which means that the capacities of these electrodes also gradually decreased with an increase in the number of charge–discharge cycles.

CV profiles of a nano-sized $Fe_2O_3$ (Aldrich, ca. 3 nm) electrode without carbon are shown in Fig. 4. The redox current of this electrode decreased rapidly with repeated cycling. Comparison of the CV results of nano-sized $Fe_2O_3$-loaded carbon (Fig. 4) and nano-sized $Fe_2O_3$ without carbon (Fig. 5) demonstrated that nano-sized $Fe_2O_3$-loaded carbon materials gave better reversible capacity than nano-sized $Fe_2O_3$ without carbon.

Fig. 6 shows the charge and discharge curves in the initial 10 cycles for nano-sized $Fe_2O_3$ and nano-sized $Fe_2O_3$-loaded carbon electrodes between 0.5 and 3.0 V, respectively. The nano-sized $Fe_2O_3$ electrode without carbon exhibited poor cyclability while nano-sized $Fe_2O_3$-loaded carbon electrode provided much better cyclability. This result is consistent with the CV results. However, all of the nano-sized $Fe_2O_3$-loaded carbon electrodes showed a large irreversible capacity in the first cycle. With further cycling, the irreversible capacity decreased rapidly and reached a small value after the first few cycles. The theoretical capacity calculated using the following equation is 1006 mAh $g^{-1}$, which corresponds to 6 L per $Fe_2O_3$.

$$6Li^+ + Fe_2O_3 + 6e \leftrightarrow 2Fe + 3Li_2O$$

The large observed excess capacity compared to the theoretical capacity in the first charge (reduction of $Fe_2O_3$) for all of the electrodes suggests that $Fe^{3+}$ was reduced to $Fe^0$ via an electrochemical reaction and/or the electrolyte underwent a reaction. For all of the nano-sized $Fe_2O_3$-loaded carbon electrodes (Fig. 6), the capacity gradually decreased with further cycling. Among the carbons used for nano-sized $Fe_2O_3$-loaded carbon electrodes, graphite and VGCF showed a large decrease in capacity upon repeated cycling compared with other carbons. This can be explained based on the morphology of carbon. When nano-carbons, such as AB, tubular CNF or platelet CNF, which have a greater surface area than graphite or VGCF, were used, $Fe_2O_3$ was more dispersed on nano-carbons, which supported the reaction of $Fe_2O_3$. This is seen in TEM images of the elec-

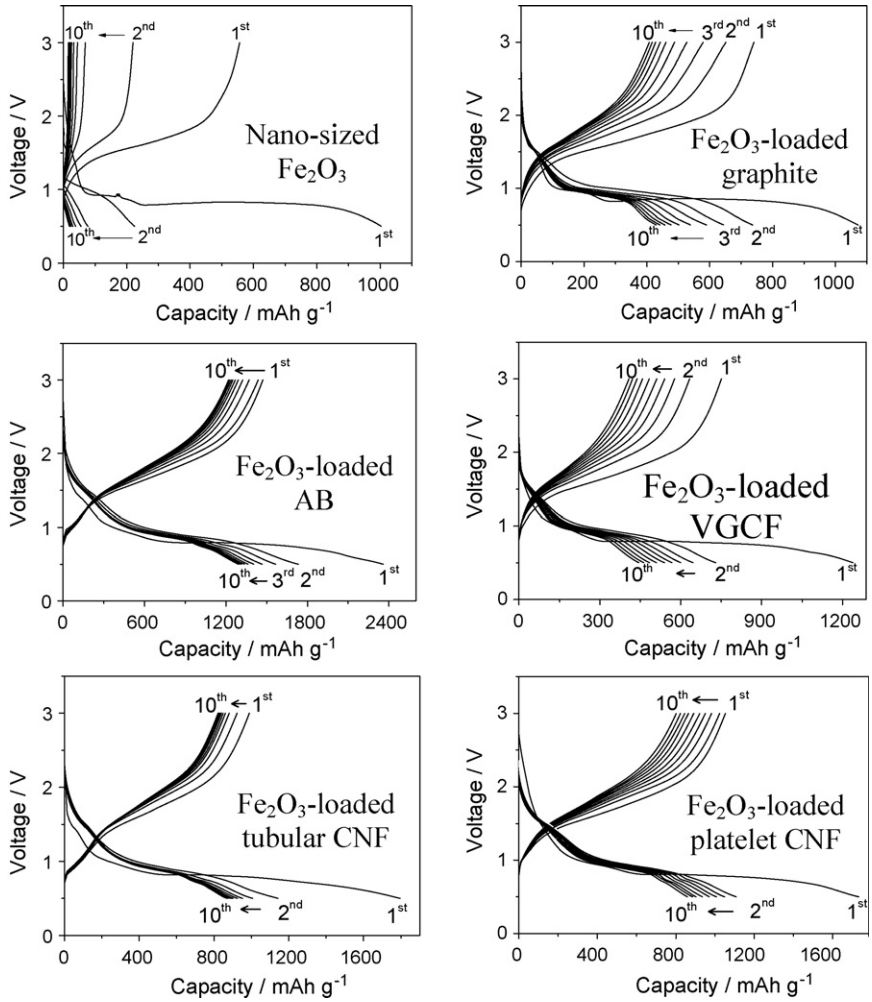


Fig. 6. Charge–discharge profiles for the 10 initial cycles for nano-sized $Fe_2O_3$ and nano-sized $Fe_2O_3$-loaded carbon electrodes.

trodes before cycling (Fig. 2), as evidenced by a smaller particle size of $Fe_2O_3$ in the case of tubular CNF compared with VGCF or graphite.

To check the valence state of iron before and after the first cycle, XPS measurements were carried out on nano-sized $Fe_2O_3$-loaded AB and graphite, and the results are presented in Figs. 7 and 8. Before cycling (Fig. 7), the sharp peak of the $Fe2p_{3/2}$ component at a binding energy of 710.9 eV is characteristic of trivalent iron ($Fe_2O_3$) [10]. After the first charge (reduction of $Fe_2O_3$) to 0.5 V at 0.2 mA cm$^{-2}$, the $Fe2p_{3/2}$ peak was shifted toward a lower binding energy at around 706.9 eV (Fig. 8). The position of this peak is consistent with iron metal reported in the Handbook of XPS [10]. In addition, a very small hump is observed at a binding energy of 710.9 eV. This result indicates that during the charge process, almost all trivalent iron is reduced to iron metal, however, a small amount of iron oxides

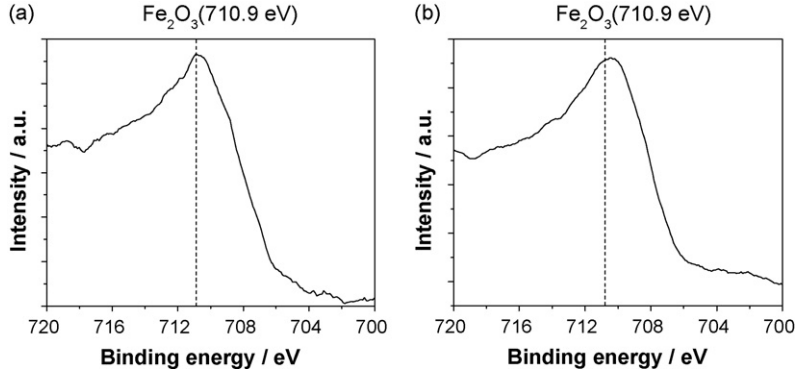


Fig. 7. XPS spectra of Fe $2p_{3/2}$ core level for nano-sized $Fe_2O_3$-loaded (a) AB and (b) graphite before cycling.

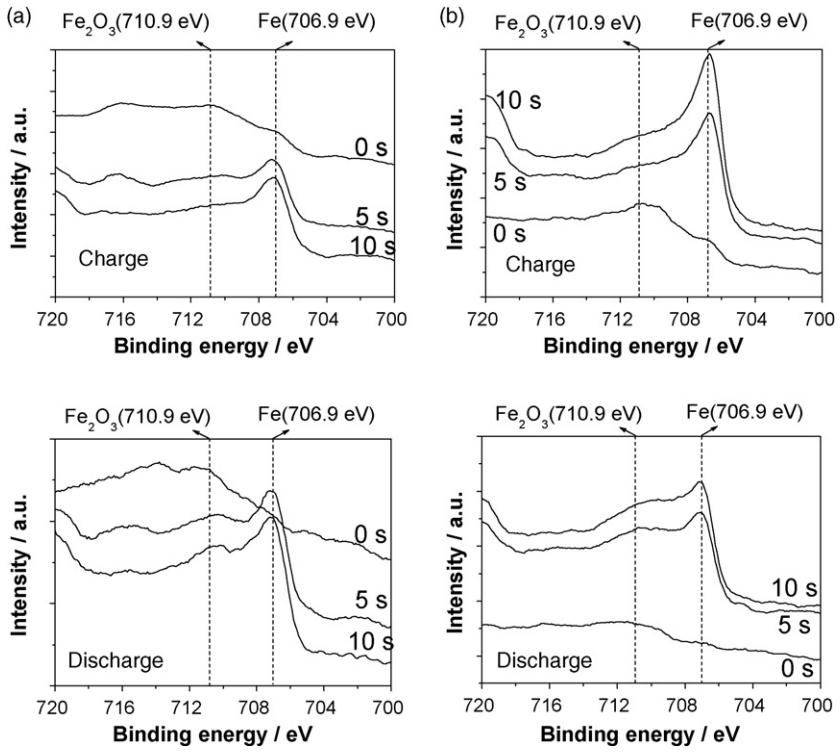


Fig. 8. XPS spectra of Fe $2p_{3/2}$ core level for nano-sized $Fe_2O_3$-loaded (a) AB and (b) graphite after the first cycle (0s, 5s, 10s: sputtering times).

still remained. Conversely, after the first discharge (oxidation Fe) to 3.0 V at 0.2 mA $cm^{-2}$, the sharp peak of the $Fe2p_{3/2}$ component at a binding energy of 706.9 eV was still observed together with the broad peak of the $Fe2p_{3/2}$ component at a binding energy of 710.9 eV (Fig. 8). These peaks are characteristic of iron metal and trivalent iron, respectively. Thus, iron metal was not oxidized completely to cause a large decrease in capacity during cycling. This may be due to the covering of non-conductive $Li_2O$, which formed during charging and inhibits the redox reaction of iron and iron oxide.

The cycle performance of all of the electrodes is presented in Fig. 9. The carbonaceous materials also contributed to the capacity of the electrode. Larcher et al. [5] showed that the reaction of lithium with carbon SP is about 60 mAh $g^{-1}$, which is small compared to the high capacity values in their work.

To determine the contribution of carbon in the present study, a carbon electrode without $Fe_2O_3$ was cycled and the results are also shown in Fig. 9. These results confirmed that the capacity caused by the reaction of lithium with carbon is very small compared to that of nano-sized $Fe_2O_3$-loaded carbon electrodes. The capacity of all the electrodes after subtracting the contribution of carbon is shown in Fig. 10. All of the electrodes showed large reversible capacities in the initial 20 cycles. However, the capacities then rapidly decreased and reached stable values. The stable specific capacities obtained are relatively small compared to those seen in the initial cycles. This may be due to the decomposition of electrolyte to form an SEI layer at the electrode surface and/or the re-distribution of iron species during cycling to result in a large decrease in capacity. Another possible explanation may involve the large difference in particle size between nano-sized $Fe_2O_3$ (a few tenths of nanometers) and carbon (Table 1) [8]. To determine the actual cause, nano-sized $Fe_2O_3$-loaded AB and tubular CNF were subjected to TEM measurements after the 10th and 50th cycles. The results are shown in Fig. 11. TEM images of cycled samples indicated that the morphology of iron and carbon species was changed compared to that before cycling (Fig. 2).

This suggests that the structure of the electrode changed during cycling, perhaps due to insufficient binder content to connect all of the pieces in the electrode. Therefore, during cycling, the electrode was destroyed, which led to a rapid decrease in capacity. On the other hand, the decrease in capacity may involve the formation of an SEI layer on the surface of the electrode. This problem will be addressed in a future study.

Comparison of the cycle performance of nano-sized $Fe_2O_3$-loaded carbon using various carbonaceous materials shows that the reversible capacity values of the electrodes that used nano-carbons such as AB, tubular CNF or platelet CNF are greater than those of electrodes that used VGCF or graphite. Among the nano-carbons used, AB provided better cycle performance after prolonged cycling. This phenomenon can be explained based on the difference in the distribution of iron oxide on the carbon surface. In the case of nano-carbons, which have a greater surface area than VGCF or graphite (see Table 1), iron oxide particles are more dispersed than on VGCF or graphite, resulting in a greater surface area of iron oxide on nano-carbons. Thereby, nano-sized $Fe_2O_3$-loaded nano-carbons provide a higher capacity than nano-sized $Fe_2O_3$-loaded VGCF or graphite. With further study,

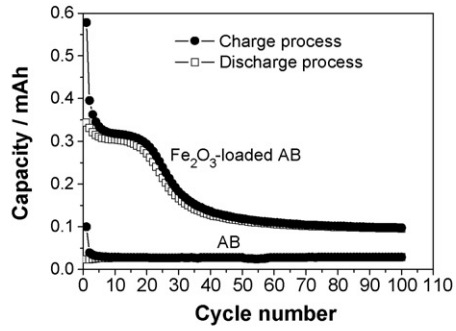


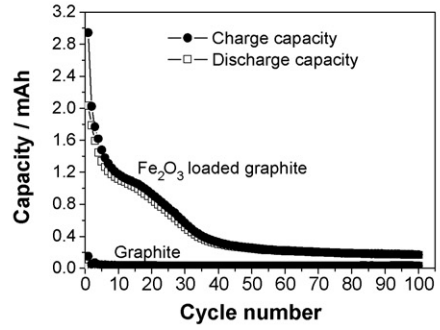


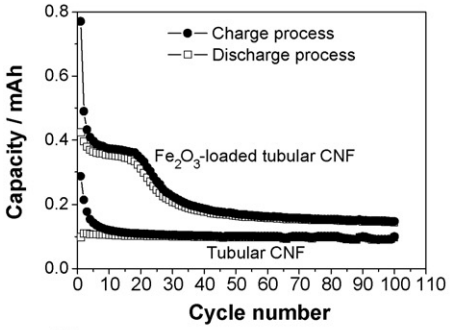


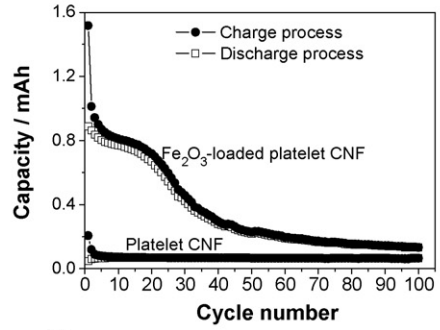


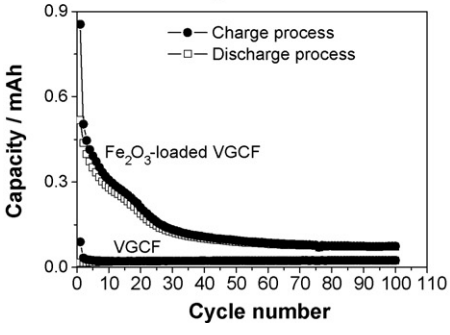


Fig. 9. Cycle performance of carbon and nano-sized $Fe_2O_3$-loaded carbon electrodes.

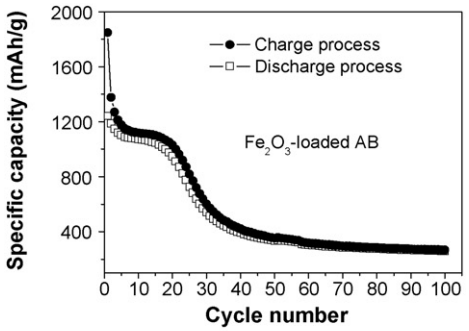


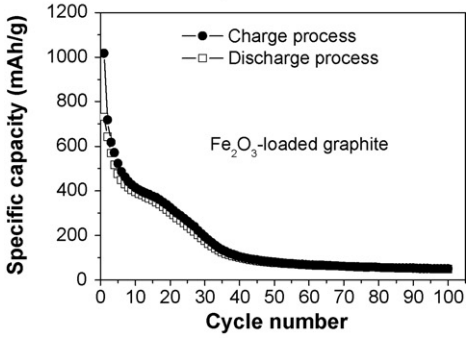


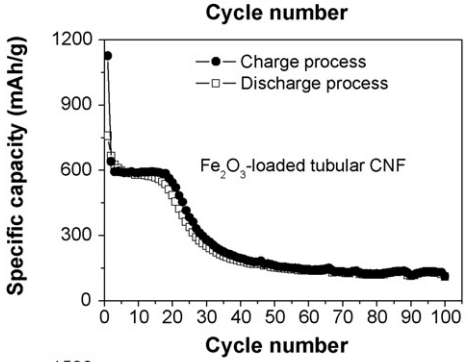


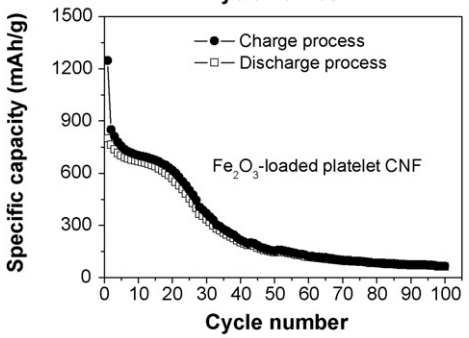


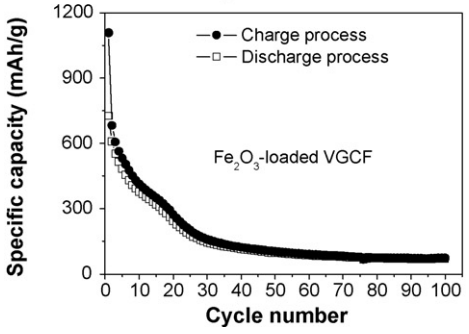


Fig. 10. Cycle performance of nano-sized $Fe_2O_3$-loaded carbon electrodes.

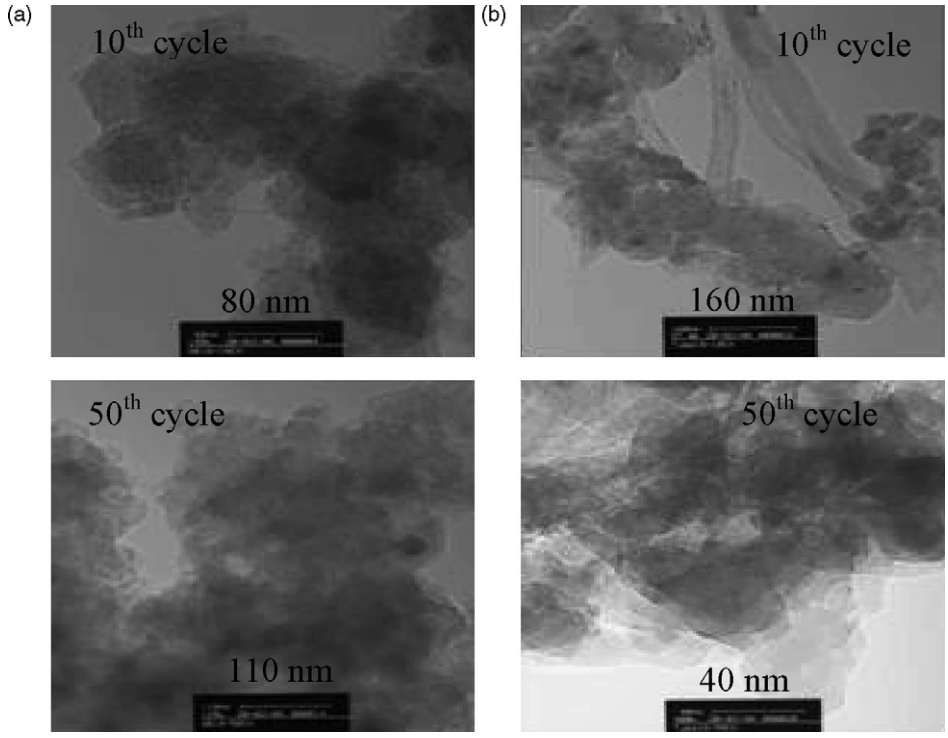


Fig. 11. TEM images of nano-sized $Fe_2O_3$-loaded (a) AB and (b) tubular CNF after the 10th and 50th cycles.

this material is expected to be a promising candidate for use in a high-capacity lithium-ion battery negative electrode.

## 4. Conclusion

Nano-sized $Fe_2O_3$-loaded carbon materials using various carbons were successfully prepared by impregnating iron nitrate on a carbon surface. Nano-sized $Fe_2O_3$-loaded carbons act as rechargeable electrode materials in a lithium cell. The high capacities observed for all of the electrodes at the first cycle suggest that $Fe^{3+}$ in $Fe_2O_3$ was reduced to $Fe^0$ via electrochemical reactions. XPS measurement confirmed this reduction during the first charge. Conversely, during the first discharge, iron was not oxidized completely. TEM images demonstrated that the structure of the electrode changed during cycling. These are the main reasons for the gradual decrease in capacity of the electrode. Although a large decrease in capacity was observed, nano-sized $Fe_2O_3$-loaded nano-carbons are promising candidates as an anode material for a lithium ion battery. With further improvements in capacity retention, nano-sized $Fe_2O_3$-loaded nano-carbons are expected to be a potential candidate for use at the anode to achieve high capacity in a lithium ion battery.

## Acknowledgement

This work was supported by the CREST program of JST (Japan Science & Technology Agency).

## References

[1] N.A. Godshall, I.D. Raistrick, R.A. Huggins, Mater. Res. Bull. 15 (1980) 561–570.
[2] M.M. Thackeray, J. Coetzer, Mater. Res. Bull. 16 (1981) 591–597.
[3] M. Pernet, P. Strobel, B. Bonnet, P. Bordet, Y. Chabre, Solid State Ionics 66 (1993) 259–265.
[4] D. Larcher, D. Bonnin, R. Cortes, I. Rivals, L. Personnaz, J.M. Tarascon, J. Electrochem. Soc. 150 (2003) A1643–A1650.
[5] D. Larcher, C. Masquelier, D. Bonnin, Y. Chabre, V. Masson, J.B. Leriche, J.M. Tarascon, J. Electrochem. Soc. 150 (2003) A133–A139.
[6] H. Morimoto, S. Tobishima, Y. Iizuka, J. Power Sources 146 (2005) 315–318.
[7] S. Ito, K. Nakaoka, M. Kawamura, K. Ui, K. Fujimoto, N. Koura, J. Power Sources 146 (2005) 319–322.
[8] S. Kanzaki, T. Inada, T. Matsumura, N. Sonoyama, A. Yamada, M. Takano, R. Kanno, J. Power Sources 146 (2005) 323–326.
[9] B.T. Hang, I. Watanabe, T. Doi, S. Okada, J. Yamaki, J. Power Sources 161 (2006) 1281–1287.
[10] Handbook of X-ray photoelectron spectroscopy (XPS) (1991) (JEOL).